

The Resolution of Chiral, Tetrahedral M_4L_6 Metal-Ligand Hosts

Anna V. Davis, Dorothea Fiedler, Marco Ziegler, Andreas Terpin, and Kenneth N. Raymond

Department of Chemistry, University of California, Berkeley, CA 94720-1460
and
Lawrence Berkeley National Laboratory, Berkeley, CA 94720

ABSTRACT The supramolecular metal-ligand assemblies of M_4L_6 stoichiometry are chiral ($M = Ga^{III}$, Al^{III} , In^{III} , Fe^{III} , Ti^{IV} , or Ge^{IV} , $H_4L = N,N'$ -bis(2,3-dihydroxybenzoyl)-1,5-diaminonaphthalene). The resolution process of $\Delta\Delta\Delta\Delta$ - and $\Lambda\Lambda\Lambda\Lambda$ - $[M_4L_6]^{12-}$ by the chiral cation *s*-nicotinium (*s*-nic⁺) is described for the Ga^{III} , Al^{III} , and Fe^{III} assemblies, and the resolution is shown to be proton dependent. From a methanol solution of $M(acac)_3$, H_4L , *s*-nicI, and KOH, the $\Delta\Delta\Delta\Delta$ - $KH_3(s\text{-}nic)_7[(s\text{-}nic) \subset M_4L_6]$ complexes precipitate, and the $\Lambda\Lambda\Lambda\Lambda$ - $K_6(s\text{-}nic)_5[(s\text{-}nic) \subset M_4L_6]$ complexes subsequently can be isolated from the supernatant. Ion exchange enables the isolation of the $(NEt_4^+)_{12}$, $(NMe_4^+)_{12}$ and K^+_{12} salts of the resolved structures, which have been characterized by CD and NMR spectroscopies. Resolution can also be accomplished with one equivalent of NEt_4^+ blocking the cavity interior, demonstrating that external binding sites are responsible for the difference in *s*-nic⁺ enantiomer interactions. Circular dichroism data demonstrate that the $(NMe_4^+)_{12}$ and $(NEt_4^+)_{12}$ salts of the resolved $[Ga_4L_6]^{12-}$ and $[Al_4L_6]^{12-}$ structures retain their chirality over extended periods of time (>20 d) at room temperature; heating the $(NEt_4^+)_{12}[Ga_4L_6]$ assembly to 75 °C also had no effect on its CD spectrum. Finally, experiments with the resolved $K_{12}[Ga_4L_6]$ assemblies point to the role of a guest in stabilizing the resolved framework.

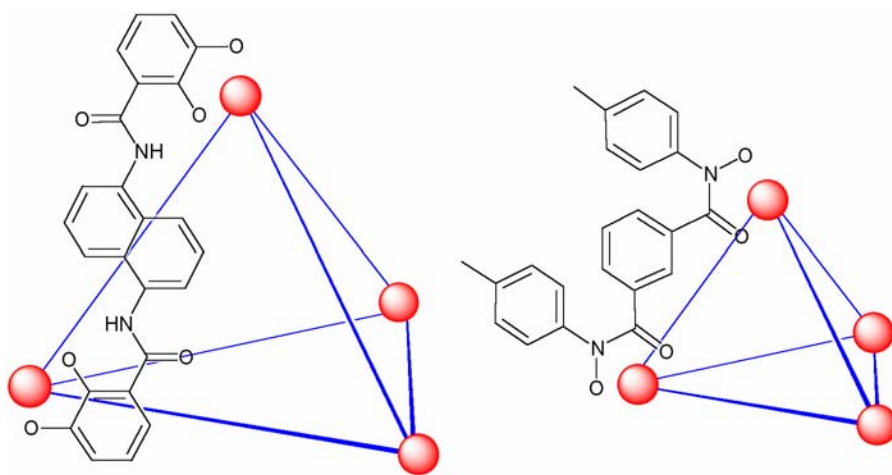


Figure 1. Schematic representations of the M_4L_6 (left) and M_4L_2 (right) tetrahedra.

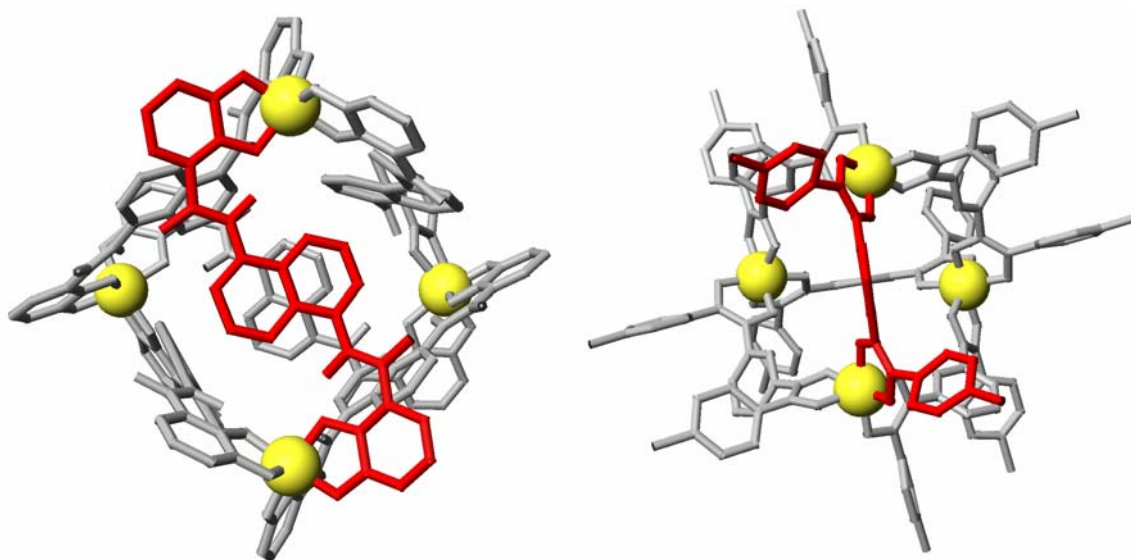


Figure 2. Crystal structures of $[\text{Fe}416]^{12-}$ and $[\text{Ga}426]^{10, 21}$. The C_2 axis is perpendicular to the ligand backbone of **1** but is in the plane of the ligand backbone of **2**.

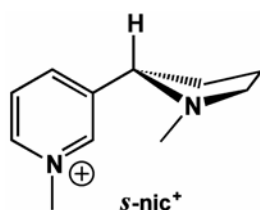


Figure 3. Chiral (*S*)-*N*-methyl-nicotinium (*s-nic*⁺) cation used in $[\text{M}416]^{12-}$ resolution.

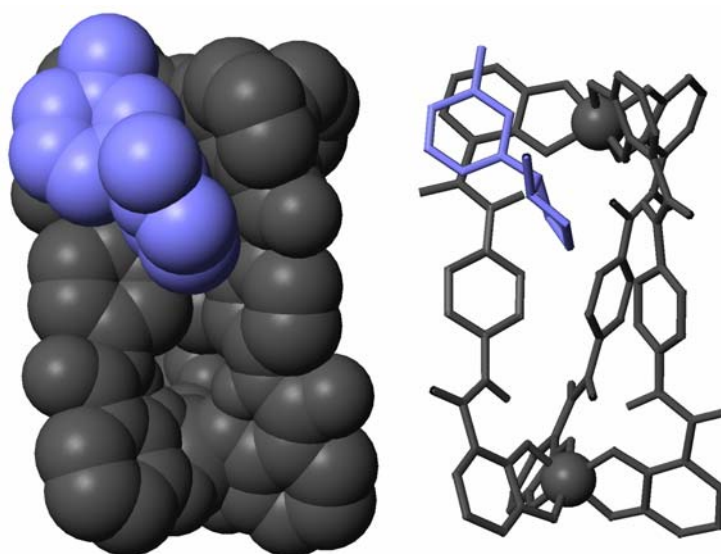


Figure 4. Space filling (left) and cylinder (right) representations of the crystal structure of $\Lambda\Lambda\text{-K}(\text{s-nic})_5[\text{Ga}233]$. For simplicity, only one *s-nic*⁺ counter ion is included.¹⁴

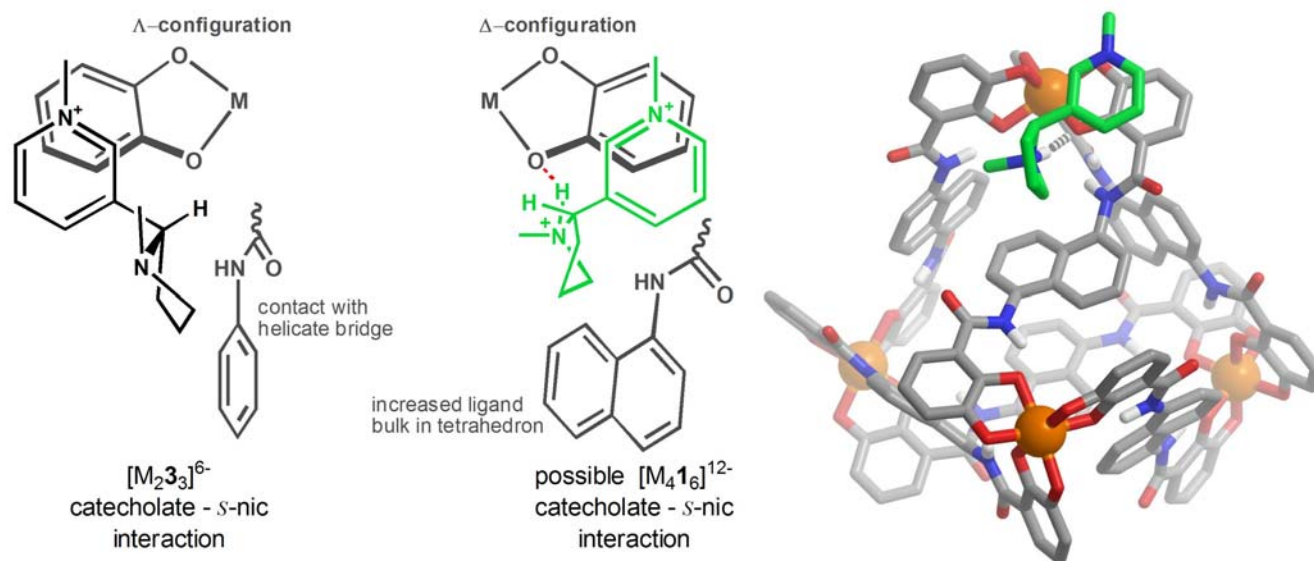


Figure 5. Left: simplified representation of the *S*-nic⁺-[M₂3₃]⁶⁻ helicate interaction. Middle: proposed *S*-nic⁺ interaction with the [M₄1₆]¹²⁻ tetrahedron which might account for pyrrolidine protonation and the differences between the steric demands of the helicate and tetrahedron ligands. A pyrrolidinium-catecholate hydrogen bond is highlighted in red. Right: Modeled *S*-nicH²⁺-[M₄1₆]¹²⁻ interaction (CACHE, MM3)²⁷, carbons of the *S*-nicH²⁺ cation are shown in green for clarity.

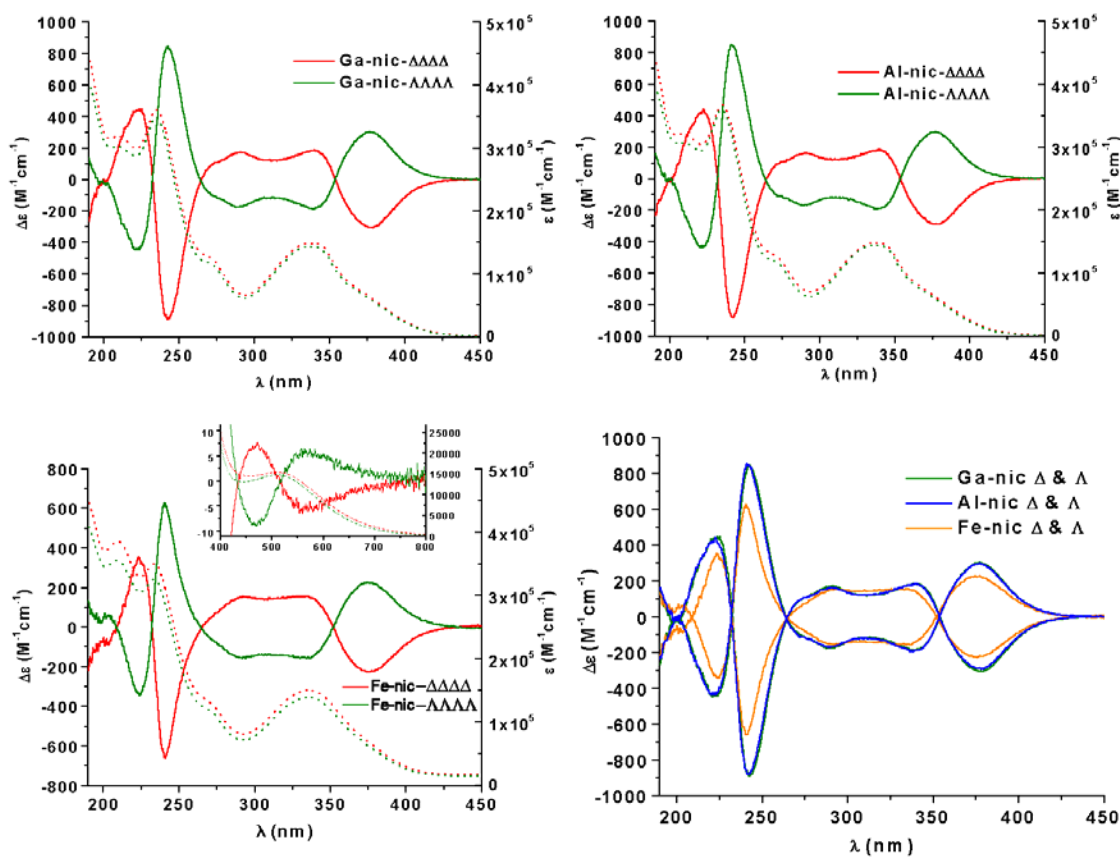


Figure 6. CD (solid lines) and UV-Vis (dotted lines) spectra of the *S*-nic⁺ salts of the resolved [Ga₄1₆]¹²⁻, [Al₄5₆]¹²⁻, and [Fe₄5₆]¹²⁻ tetrahedral assemblies.

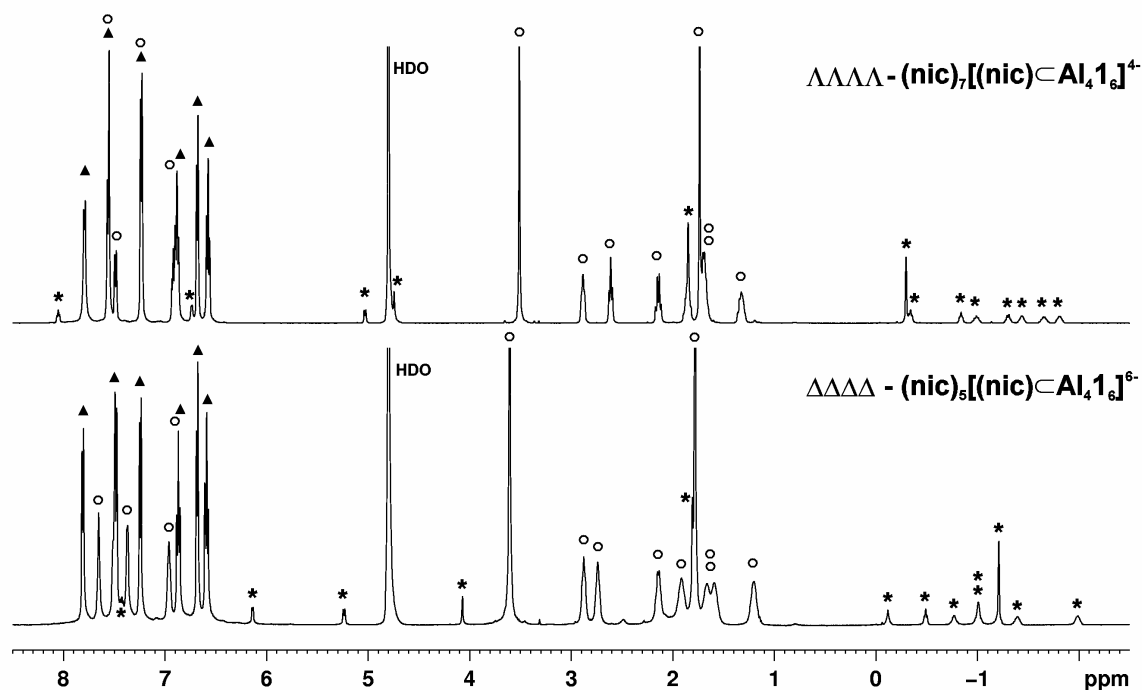


Figure 7. ^1H NMR (500 MHz, D_2O) spectra of the $\Lambda\Lambda\Lambda\Lambda-(S\text{-nic})_7[(S\text{-nic}) \subset \text{Al}_4\mathbf{1}_6]^{4-}$ and $\Delta\Delta\Delta\Delta-(S\text{-nic})_5[(S\text{-nic}) \subset \text{Al}_4\mathbf{1}_6]^{6-}$ complexes. (\blacktriangle = host; \circ = exterior $S\text{-nic}^+$; * = encapsulated $S\text{-nic}^+$)

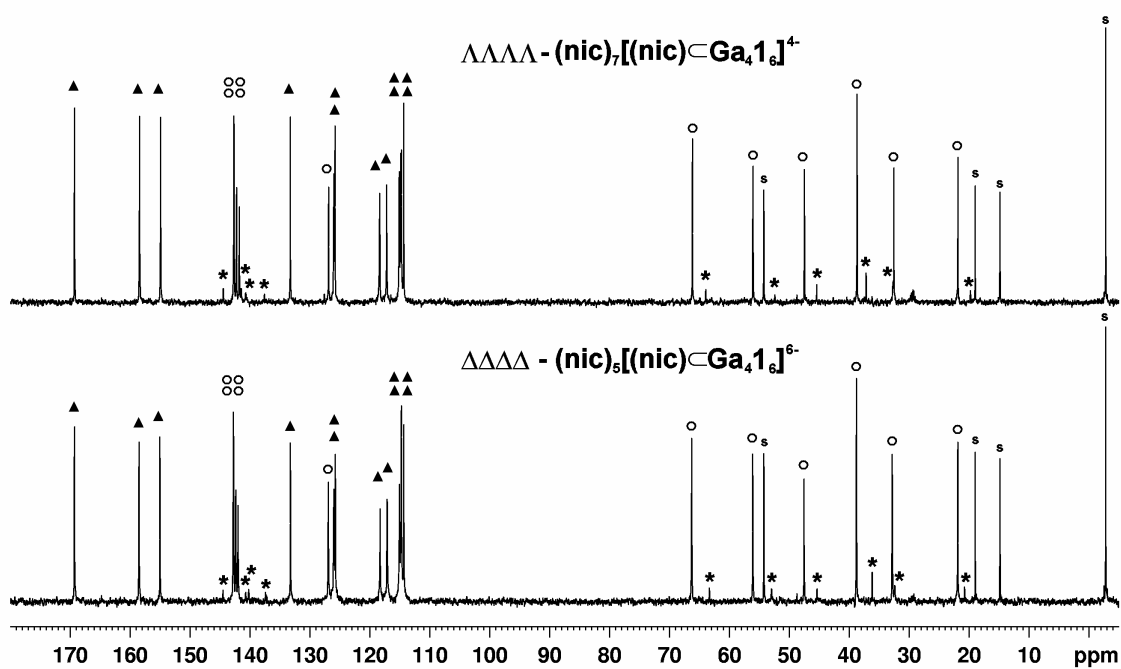


Figure 8. ^{13}C NMR (100 MHz, D_2O) spectra of $\Lambda\Lambda\Lambda\Lambda-(S\text{-nic}^+)_7[(S\text{-nic}^+) \subset \text{Ga}_4\mathbf{1}_6]^{4-}$ and $\Delta\Delta\Delta\Delta-(S\text{-nic})_5[(S\text{-nic}) \subset \text{Ga}_4\mathbf{1}_6]^{6-}$. (\blacktriangle = host; \circ = exterior $S\text{-nic}^+$; * = encapsulated $S\text{-nic}^+$, s = internal standard)

Table 1. ^1H NMR data for $S\text{-nic}^+ [\text{M}_4\text{L}_6]^{12-}$ compounds. (500 MHz, D_2O)				
^1H NMR	Ga $\Delta\Delta\Delta\Delta$	Ga $\Delta\Delta\Delta\Delta$	Al $\Delta\Delta\Delta\Delta$	Al $\Delta\Delta\Delta\Delta$
Host Ar(H)				
naphthyl- <i>H</i>	7.81 (d, $J = 7.6$, 12H)	7.79 (d, $J = 7.5$, 12H)	7.81 (d, $J = 7.6$, 12H)	7.79 (d, $J = 7.0$, 12H)
naphthyl- <i>H</i>	7.49 (d, $J = 8.4$, 12H)	7.55 (d, $J = 8.5$, 12H)	7.48 (d, $J = 8.7$, 12H)	7.56 (d, $J = 8.7$, 12H)
catechol- <i>H</i>	7.28 (d, $J = 8.4$, 12H)	7.27 (d, $J = 8.4$, 12H)	7.24 (d, $J = 8.2$, 12H)	7.23 (d, $J = 7.6$, 12H)
naphthyl- <i>H</i>	6.84 (t, $J = 8.0$, 12H)	6.85 (t, $J = 7.9$, 12H)	6.86 (t, $J = 8.0$, 12H)	6.88 (t, $J = 7.4$, 12H)
catechol- <i>H</i>	6.75 (d, $J = 7.3$, 12H)	6.76 (d, $J = 7.3$, 12H)	6.68 (d, $J = 7.3$, 12H)	6.68 (d, $J = 7.1$, 12H)
catechol- <i>H</i>	6.59 (t, $J = 7.6$, 12H)	6.58 (t, $J = 7.3$, 12H)	6.59 (t, $J = 8.0$, 12H)	6.58 (t, $J = 7.3$, 12H)
$S\text{-nic}^+$ (exterior)				
pyridinium- <i>H</i>	7.67 (s, 7H)	7.56 (s, 5H)	7.65 (s, 7H)	7.55 (s, 5H)
pyridinium- <i>H</i>	7.53 (d, $J = 7.9$, 7H)	7.50 (d, $J = 8.0$, 5H)	7.49 (br m, 7H)	7.50 (d, $J = 8.0$, 5H)
pyridinium- <i>H</i>	7.42 (d, $J = 5.2$, 7H)	7.29 (d, $J = \text{n.d.}$, 5H)	7.36 (br m, 7H)	7.23 (d, $J = \text{n.d.}$, 5H)
pyridinium- <i>H</i>	6.97 (t, $J = 6.6$, 7H)	6.94 (t, $J = 6.8$, 5H)	6.96 (br m, 7H)	6.92 (t, $J = 6.5$, 5H)
pyridinium- NCH_3	3.61 (s, 21H)	3.51 (s, 15H)	3.61 (s, 21H)	3.51 (s, 15H)
pyrrolidine- <i>H</i>	2.88 (t, $J = 8.3$, 7H)	2.88 (br m, 5H)	2.88 (br m, 7H)	2.88 (br m, 5H)
pyrrolidine- <i>H</i>	2.75 (t, $J = 8.1$, 7H)	2.60 (t, $J = 8.3$, 5H)	2.74 (br m, 7H)	2.61 (t, $J = 8.1$, 5H)
pyrrolidine- <i>H</i>	2.14 (q, $J = 9.0$, 7H)	2.13 (q, $J = 8.9$, 5H)	2.14 (br m, 7H)	2.14 (q, $J = 8.7$, 5H)
pyrrolidine- <i>H</i>	1.92 (br m, 7H)	1.82 (br m, 5H)	1.91 (br m, 7H)	1.86 (br m, 5H)
pyrrolidine- NCH_3	1.79 (s, 21H)	1.73 (s, 15H)	1.78 (s, 21H)	1.73 (s, 15H)
pyrrolidine- <i>H</i>	1.66 (br m, 7H)	1.69 (br m, 10H)	1.66 (br m, 7H)	1.69 (br m, 10H)
pyrrolidine- <i>H</i>	1.59 (br m, 7H)	1.32 (br m, 5H)	1.59 (br m, 7H)	1.33 (br m, 5H)
pyrrolidine- <i>H</i>	1.20(br m, 7H)		1.20(br m, 7H)	
$S\text{-nic}^+$ (encapsulated)				
pyridinium- <i>H</i>	7.35 (t, $J = 6.2$, 1H)	7.93 (t, $J = 6.2$, 1H)	7.42 (t, $J = 6.9$, 1H)	8.05 (t, $J = 6.20$, 1H)
pyridinium- <i>H</i>	6.16 (d, $J = 4.9$, 1H)	6.71 (d, $J = 5.2$, 1H)	6.14 (t, $J = 5.1$, 1H)	6.73 (d, $J = 5.0$, 1H)
pyridinium- <i>H</i>	5.23 (d, $J = 7.6$, 1H)	5.02 (d, $J = 7.7$, 1H)	5.24 (d, $J = 7.8$, 1H)	5.03 (d, $J = 7.9$, 1H)
pyridinium- <i>H</i>	4.11 (s, 1H)	4.72 (s, 1H)	4.07 (s, 1H)	4.74 (s, 1H)
pyridinium- NCH_3	1.81 (s, 3H)	1.83 (s, 3H)	1.81 (s, 3H)	1.85 (s, 3H)
pyrrolidine- <i>H</i>	-0.07 (br m, 1H)	-0.34 (br m, 1H)	-0.12 (br m, 1H)	-0.30 (s, 3H)
pyrrolidine- <i>H</i>	-0.47 (t, $J = 7.2$, 1H)	-0.37 (s, 3H)	-0.49 (t, $J = 7.7$, 1H)	-0.34 (t, $J = 7.3$, 1H)
pyrrolidine- <i>H</i>	-0.76 (br m, 1H)	-0.77 (br m, 1H)	-0.77 (br m, 1H)	-0.84 (br m, 1H)
pyrrolidine- <i>H</i>	-0.97 (br m, 2H)	-0.98 (br m, 1H)	-1.01 (br m, 2H)	-0.99 (br m, 1H)
pyrrolidine- NCH_3	-1.16 (s, 3H)	-1.27 (br m, 1H)	-1.21 (s, 3H)	-1.14 (br m, 1H)
pyrrolidine- <i>H</i>	-1.34 (br m, 1H)	-1.40 (br m, 1H)	-1.39 (br m, 1H)	-1.30 (br m, 1H)
pyrrolidine- <i>H</i>	-1.96 (br m, 1H)	-1.62 (br m, 1H)	-1.99 (br m, 1H)	-1.66 (br m, 1H)
pyrrolidine- <i>H</i>		-1.81 (br m, 1H)		-1.81 (br m, 1H)
^1H Chemical shifts are referenced to a sodium 3-(trimethylsilyl)-propane sulfonate internal standard.				

Table 2. ^{13}C NMR data for <i>S</i> -nic ⁺ [M ₄ 1 ₆] ¹²⁻ compounds. (100 MHz, D ₂ O)				
^{13}C NMR	Ga ΔΔΔΔ	Ga ΛΛΛΛ	Al ΔΔΔΔ	Al ΛΛΛΛ
Host				
carbonyl-CO	170.0	170.0	170.0	170.0
catechol-CO	159.2	159.1	160.2	160.1
catechol-CO	155.7	155.6	156.9	156.7
catechol-C	134.0	134.0	134.0	134.0
catechol-C	126.8	126.8	126.7	126.7
catechol-C	126.5	126.6	126.5	126.6
naphthyl-C	119.1	119.1	119.1	119.3
naphthyl-C	117.9	118.0	117.9	118.0
naphthyl-C	115.8	115.9	115.7	115.7
naphthyl-C	115.7	115.6	115.5	115.5
naphthyl-C	115.5	115.5	114.7	114.8
Naphthyl-C	115.1	115.5	114.6	114.6
<i>S</i> -nic ⁺ (ext)				
pyrid.-C	143.6	143.5	143.5	143.4
pyrid.-C	143.4	143.4	143.4	143.2
pyrid.-C	143.1	143.0	143.2	142.9
pyrid.-C	142.8	142.5	142.8	142.5
pyrid.-C	127.7	127.7	127.7	127.6
pyrid.-NCH ₃	67.1	66.9	67.1	66.9
pyrol.-C	56.9	56.8	56.9	56.8
pyrol.-C	48.3	48.2	48.3	48.3
pyrol.-NCH ₃	39.6	39.4	39.6	39.5
pyrol.-C	33.6	33.3	33.6	33.3
pyrol.-C	22.7	22.6	22.7	22.6
<i>S</i> -nic ⁺ (enc.)				
pyrid.-C	145.3	145.2	145.2	145.2
pyrid.-C	142.7	142.2	142.7	142.3
pyrid.-C	141.5	141.5	140.9	141.5
pyrid.-C	141.0	138.4	138.1	138.3
pyrid.-C	127.6	128.4	128.2	128.6
pyrid.-NCH ₃	64.1	64.7	64.0	64.6
pyrol.-C	53.7	53.2	53.7	53.1
pyrol.-C	46.1	46.2	46.1	46.2
pyrol.-NCH ₃	37.0	37.9	37.0	38.2
pyrol.-C	33.1	33.4	33.0	33.5
pyrol.-C	21.5	20.6	21.6	20.6
¹³ C Chemical shifts are referenced to a sodium 3-(trimethylsilyl)-propane sulfonate internal standard.				

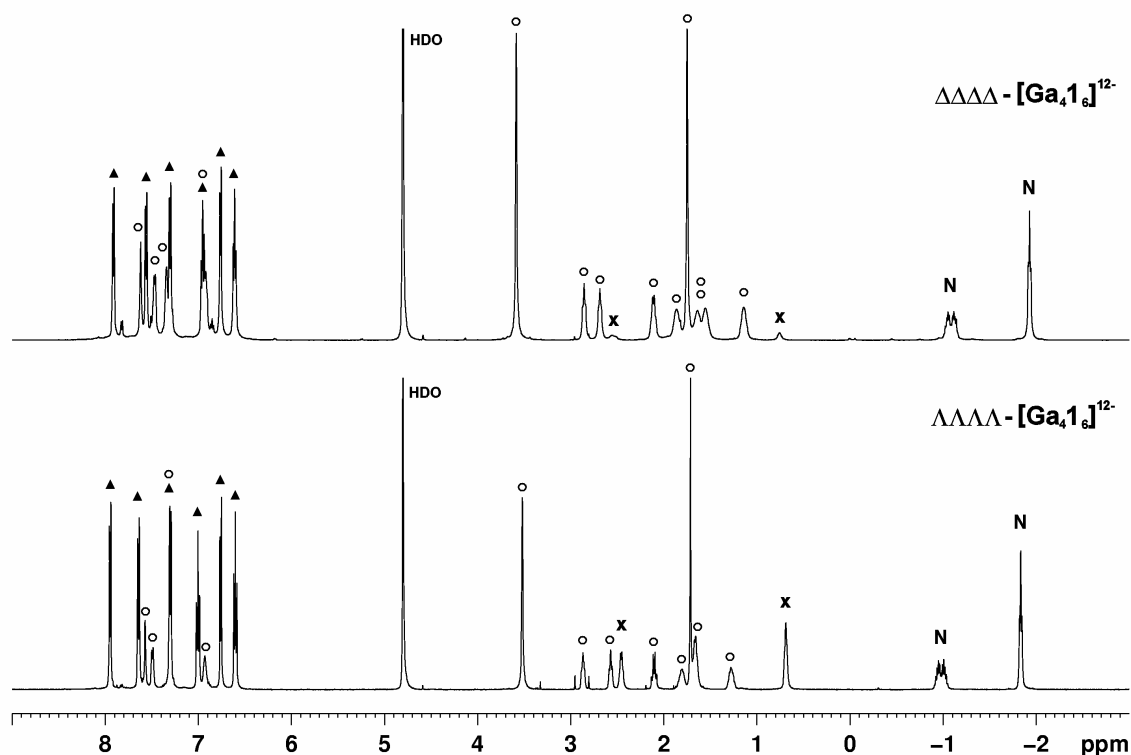


Figure 9. ^1H NMR (500 MHz, D_2O) of the $s\text{-nic}^+$ salts of the resolved $[(\text{NEt}_4)\text{Ga}_4\mathbf{1}_6]^{11-}$ enantiomers. (\blacktriangle = host; \circ = exterior $s\text{-nic}^+$; N = encapsulated NEt_4^+ , x = external NEt_4^+)

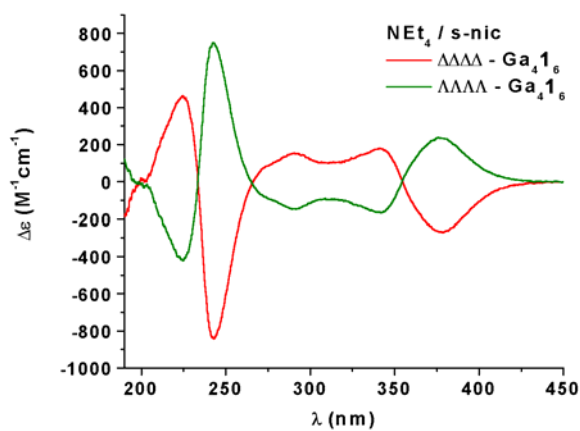


Figure 10. CD spectra of the $s\text{-nic}^+$ salts of the resolved $[(\text{NEt}_4)\text{Ga}_4\mathbf{1}_6]^{11-}$ enantiomers.

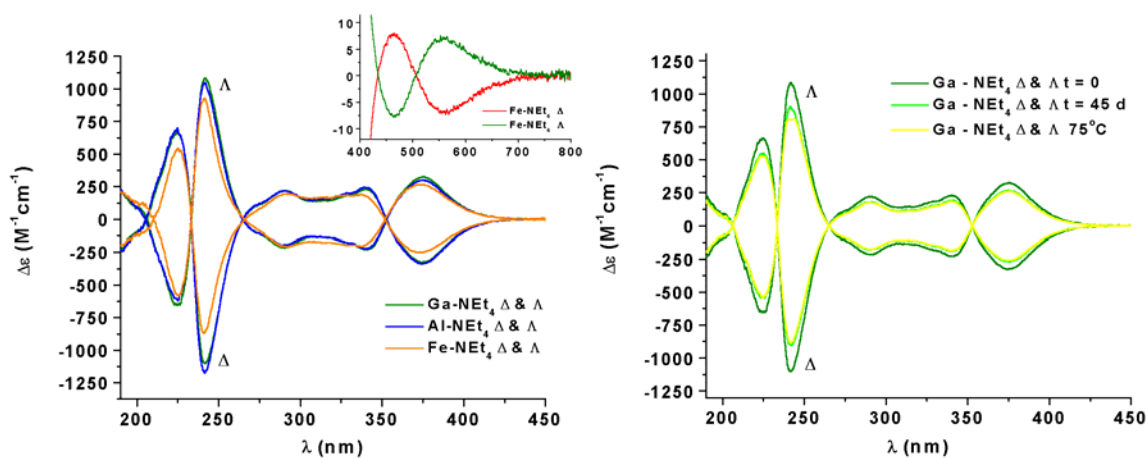


Figure 11. Left: CD spectra of the NEt_4^+ salts of the $\Delta\Delta\Delta\Delta$ - and $\Lambda\Lambda\Lambda\Lambda$ - enantiomers of $[\text{Ga}_4\mathbf{1}_6]^{12-}$, $[\text{Al}_4\mathbf{1}_6]^{12-}$ and $[\text{Fe}_4\mathbf{1}_6]^{12-}$. Right: CD spectra of the Ga^{III} compounds taken immediately after preparation of the 0.5 mM solution, after 45 days, and then after 24 h of heating to 75 °C.

Table 3. Summary of $[\text{M}_4\mathbf{1}_6]^{12-}$ CD data

Complex	Ga^{III}	Al^{III}	Fe^{III}
$\Delta\Delta\Delta\Delta$ - (S-nic) $_6$ $[\text{M}_4\mathbf{1}_6]^{6-}$	225 (+448); 242 (-889); 291 (+173); 340 (+187); 379 (-306)	223 (+443); 242 (-883); 290 (+165); 339 (+187); 378 (-292)	223 (+356); 241 (-659); 292 (+155); 339 (+146); 376 (+228); 468 (+7); 565 (-6)
$\Lambda\Lambda\Lambda\Lambda$ - (S-nic) $_6$ $[\text{M}_4\mathbf{1}_6]^{4-}$	221 (-448); 243 (+848); 288 (-177); 339 (-190); 377 (+304)	221 (-437); 241 (+854); 288 (-170); 337 (-194); 377 (+298)	224 (-344); 241 (+627); 292 (-157); 337 (-159); 375 (+228); 468 (-8); 565 (+6)
$\Delta\Delta\Delta\Delta$ - (NEt $_4$) $_{12}$ $[\text{M}_4\mathbf{1}_6]$	225 (+664); 241 (-1102); 290 (+223); 340 (+230); 375 (-329)	225 (+701); 242 (-1173); 290 (+219); 339 (245); 375 (-339)	225 (+544); 241 (-869); 293 (+198); 337 (+191); 374 (-253); 465 (8); 560 (-7)
$\Lambda\Lambda\Lambda\Lambda$ - (NEt $_4$) $_{12}$ $[\text{M}_4\mathbf{1}_6]$	225 (-655); 242 (+1086); 290 (-216); 341 (-230); 375 (+330)	225 (-620); 242 (+1050); 289 (-197); 341(-225); 376 (+302)	225 (-583); 241 (+927); 292 (-212); 337 (-204); 371 (+267); 465 (-8); 560 (+7)
$\Delta\Delta\Delta\Delta$ - (NMe $_4$) $_{12}$ $[\text{M}_4\mathbf{1}_6]$	222 (+485); 241 (-870); 289 (+173); 338 (+194); 372 (-265)	n.d.	n.d.
$\Lambda\Lambda\Lambda\Lambda$ - (NMe $_4$) $_{12}$ $[\text{M}_4\mathbf{1}_6]$	223 (-473); 241 (+850); 288 (-179); 337 (-192); 373 (+267)	n.d.	n.d.

Samples concentrations were 0.5 mM and were prepared in 5 mM KOH solution. (n.d. = not determined)

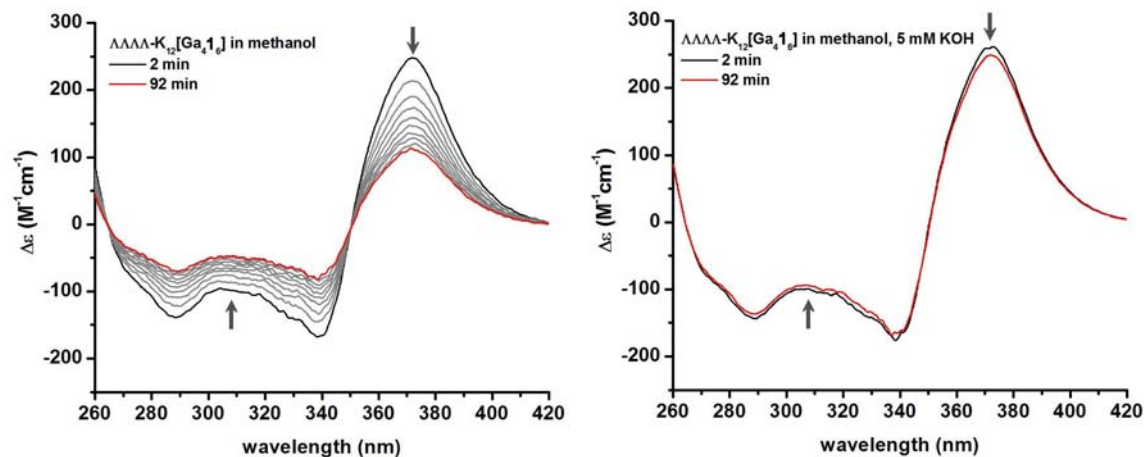


Figure 12. Left: CD spectra of $\Lambda\Lambda\Lambda\Lambda\text{-K}_{12}[\text{Ga}_4\mathbf{1}_6]$, monitored in MeOH at 10 min intervals. Right: CD spectra of $\Lambda\Lambda\Lambda\Lambda\text{-K}_{12}[\text{Ga}_4\mathbf{1}_6]$ in MeOH with 5 mM KOH. Spectra were recorded at 10 minute intervals.

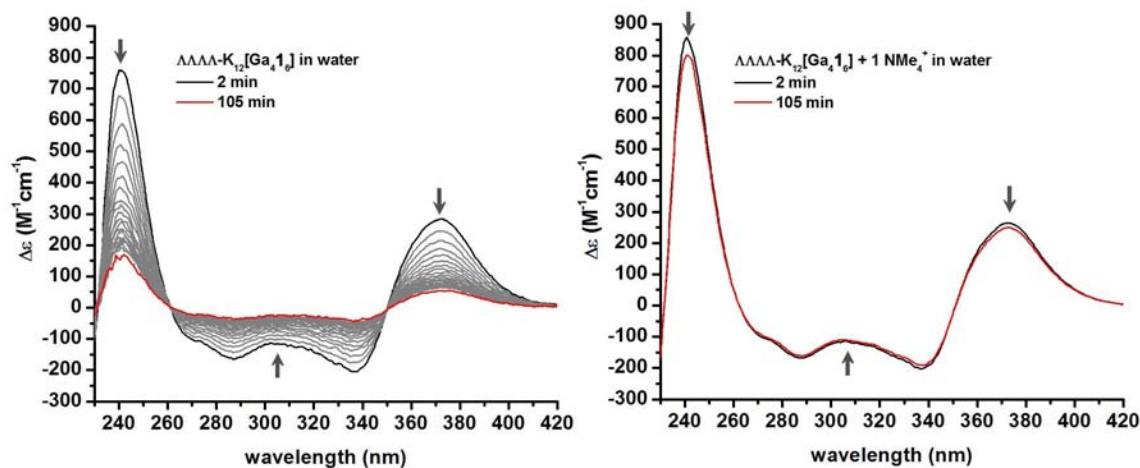


Figure 13. Left: CD spectra of $\Lambda\Lambda\Lambda\Lambda\text{-K}_{12}[\text{Ga}_4\mathbf{1}_6]$, monitored at neutral pH in H_2O . Spectra were taken in 5 minute intervals. Right: CD spectra of $\Lambda\Lambda\Lambda\Lambda\text{-K}_{12}[\text{Ga}_4\mathbf{1}_6]$ in the presence of one equivalent of NMe_4^+ , monitored at neutral pH in H_2O .

SYNOPSIS TOC Figure:

